



Article

Aquifer Response to Estuarine Stream Dynamics

Yehuda Shalem ^{1,2,3,*} , Yoseph Yechieli ^{2,4}, Barak Herut ³  and Yishai Weinstein ¹¹ Department of Geography and Environment, Bar-Ilan University, Ramat-Gan 52900, Israel² Geological Survey of Israel, Yesha'ayahu Leibowitz 32, Jerusalem 9692100, Israel³ Israel Oceanographic and Limnological Research, Tel-Shikmona, Haifa 31080, Israel⁴ Department of Environmental Hydrology & Microbiology, Ben Gurion University, Sede Boker 8499000, Israel

* Correspondence: ye.sha@live.biu.ac.il

Received: 12 June 2019; Accepted: 8 August 2019; Published: 13 August 2019



Abstract: While seawater intrusions are widely discussed, the salinization of coastal aquifers via narrow rivers is hardly documented. This study investigates groundwater dynamics in an aquifer next to an estuarine stream on the eastern Mediterranean coast. Groundwater levels and salinization patterns were examined as a response to dynamic changes in estuary water, both in low- and high-permeability aquifer units. In the high-permeability unit, the extent of salinization was relatively constant, reaching a distance of at least 80 m from the river, with no long-term changes in fresh-saline interface depth, indicating that the system is in a quasi-steady state. Groundwater salinity in the low-permeability unit showed frequent and large fluctuations (up to 36 and 22 at 5 and 20 m from the river, respectively). We suggest that the river may have a more immediate impact on a low-permeability than on a high-permeability aquifer. This is dependent on the history of seawater encroachments to the river, which are better preserved in the low-permeability unit, and on the hydrogeology of this unit, where sand lenses can serve as high-permeability conduits. However, this unit can efficiently prevent a large extent of salinization of the regional coastal aquifer by the estuary water.

Keywords: estuarine river; seawater intrusion; fresh–saline water interface; surface–groundwater interaction; permeability

1. Introduction

Groundwater is an essential freshwater resource in many coastal areas. Optimal management of coastal aquifers is becoming increasingly important due to population growth and climate change, which potentially affects water quality, ecosystem health and diversity, and water-supply reliability [1–5]. Surface water and groundwater are intrinsically linked systems [6–9]. Areas around streams, rivers, lakes and coastal environments represent zones of interaction and transition between the two systems, where dissolved constituents such as pollutants can be diluted, exchanged, transformed, or degraded. Identifying predominant processes affecting solute exchange across transition zones is, therefore, critical [10–12].

The problem of seawater intrusion into coastal aquifers is widely recognized for its importance with regard to water resource management and planning in coastal areas [10,12,13]. The configuration of the seawater intrusion and its extent are determined by hydraulic gradients and by spatial variation in the hydraulic conductivity of coastal aquifers [10]. For hydrogeologically homogeneous systems, fairly reliable predictions can be made on the basis of the Ghyben–Herzberg relationship. The extent of seawater intrusion into the coastal aquifer can also be estimated by salinity measurements in observation wells [14–18] or by hydrological modeling [15,19–22], as well as by geophysical measurements [14,23,24]. While the nature of the seawater–groundwater interface was widely discussed in different coastline

settings (e.g., References [10,25] and the references therein) [26–29], the salinization of coastal aquifers via estuarine streams was hardly studied in the field [14,16,30,31].

The rate at which water exchanges between surface water and the aquifer is controlled by hydraulic gradient and sediment permeability. In rivers and estuaries, this exchange is also known as a hyporheic exchange [31–34]. Groundwater–surface water interaction in the estuarine environment is influenced by density contrasts between the typically fresh groundwater and saline-to-brackish estuarine water, which leads to convective circulation in the aquifer [7,19,35–37]. Circulation occurs even if the hydraulic gradient in the aquifer dips toward the estuary [31,38]. The size of the resultant salt wedge is dependent on the hydraulic gradient, aquifer conductivity, and estuary salinity [31,36,39].

In this paper, we investigate the dynamics and mechanisms of aquifer salinization next to a bar-built estuarine river by integrating high-resolution level and salinity measurements in the river and the adjacent aquifer.

The Study Area

The Alexander River is a perennial river on the Mediterranean coast of Israel (Figure 1a). The drainage area of the Alexander River is relatively small (555 km², Figure 1a) and, thus, it experiences relatively small peak discharges (up to ~180 m³/s in recent years; data from the Hydrological Service of Israel). Although it is a perennial river, the river's natural flow to the sea is insignificant during the dry season (the base flow entering the estuarine part is typically ≤ 0.3 m³/s), which is mostly composed of effluents from sewage treatment plants and aquaculture drainage [40].

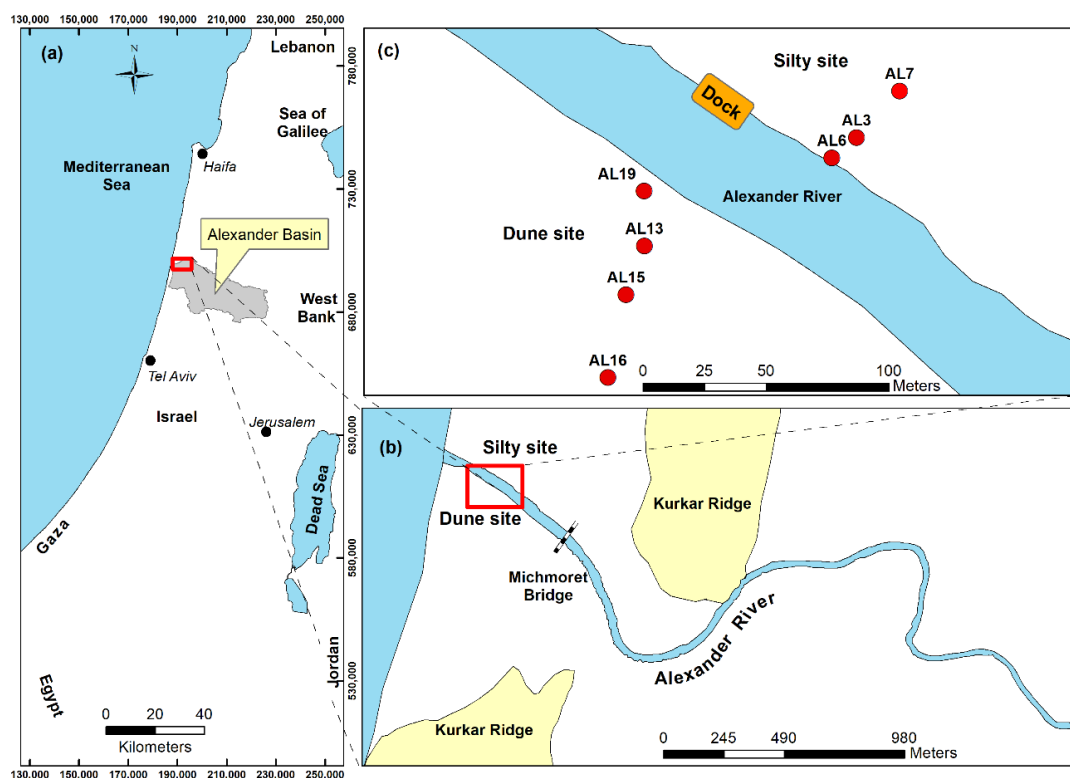


Figure 1. Maps of the study sites: (a) location map; (b) Alexander River area; (c) study site area. “Kurkar” is the local name for lithified calcareous sandstone.

The Alexander River channel cuts through two ridges of Pleistocene calcareous sandstone (locally named Kurkar) at ca. 250 and 1700 m from the sea. Between these two ridges, the river meanders in clayey layers of swamp origin [41]. West of the western ridge, the river runs through a brown-red sandy soil and coastal sand dunes, which cover Kurkar layers [42]. Due to the heterogeneous nature of

the fluvial environment, the lithological sequence frequently varies in type and thickness along the river channel.

The lower reach of the river (5.5 km from the sea; Figure 1b) is a bar-built estuary, with a typical water depth of less than 2.5 m, and with its riverbed up to ~1.6 m below sea level [40]. The connection of the river with the sea is usually blocked by a shallow bar, which is built of sand and pebbles [40,43]. The sandbar exists at the river mouth almost year-long, although it is occasionally breached, mostly during high-sea and high-discharge winter events [16].

In areas where the riverbed is below sea level, it is subjected to seawater encroachment, reaching 4–5 km upstream. As a result, the river usually develops a halo-stratified water column with saline water at the bottom and relatively fresh water at the surface. Salinities in the deep water are usually lower than 15 (compared to 39 of eastern Mediterranean seawater). Large flow rates in the deep water are usually limited to big flood events, which destroy the sandbar at the river mouth, or to high-sea conditions. Immediately after such an event, large volumes of seawater penetrate the river channel. In these cases, salinities in the deeper layer may increase to 35 and a sharp halocline is developed, which further prevents vertical mixing of surface and bottom water [16,40].

The dynamics of interaction between the river and the aquifer was studied in two close-to-sea sites (<500 m from the river mouth), north and south of the river (~300 and 250 m from the sea, respectively; Figure 1c). The northern site (hereafter the Silty site) is covered by a clayey silt unit, up to 4 m thick next to the river. The silt is underlain by the regional sandy aquifer, which is exposed 45 m from the riverbank. The clayey silt unit includes several thin sandy (~35% sand) lenses, some containing up to 70% of the mineral quartz. The southern site (hereafter the Dune site; Figure 1c) is mostly characterized by sands (50–100%; Table 1), which are separated at a depth of ~8 m by a thin (1 m) clayish silty layer (65% silt) from the regional sand aquifer. The lithology of both sites is described in detail in Shalem et al. (2014) [16].

Table 1. Grain size and hydraulic conductivities in the two sites included in this study.

Site	Lithology	Borehole	Depth (m)	Sand (%)	Silt (%)	Clay (%)	Hydraulic Conductivities (m/day) *
Silty	Clayey silt	AL6	2–3	37.0	49.0	14.0	1
Dune	Sand	AL13	3–4	94.5	5.0	0.5	13
Dune	Sand	AL15	6–7	94	5.5	0.5	15

* Hydraulic conductivities were calculated from slug tests.

2. Methods

River water and groundwater level and salinity were measured both manually and continuously by level loggers (1-h resolution) from November 2012 through November 2013. River water was monitored at two stations for water level and salinity (EC). The first station was located 250 m from the sea on a dock at the northern bank (Figure 1c). The second station was located 500 m from the sea, at the base of the Michmoret Bridge (Figure 1b). Three boreholes were drilled at the Silty site, north of the river ca. 300 m from the sea, and four boreholes were drilled at the Dune site, south of the river ~250 m from the sea (Figure 1c). Drilling methodology and locations were described in detail in Shalem et al. (2014).

Water levels were measured continuously using level loggers (Solinst Canada Ltd. Model 3001, Georgetown, Canada, respectively). Manual measurements included water level by Solinst Model 101 Water Level Meter and electrical conductivity (EC) and temperature by a DELTA-OHM HD2156.2 meter or by an LTC levelogger (Solinst Canada Ltd., Model 3001, Georgetown, Canada). Salinity was calculated from the EC and temperature values, using the practical 1978 salinity scale (PSU) [44]. Manual salinity profile measurements were conducted (in the river and some boreholes) 13 times during the study period. Because the salinity profile revealed that there is a fresh–saline interface in

the Dune site, groundwater salinities in the Dune site were continuously monitored at two depths, just above and below the interface.

Regional groundwater levels were taken from databases of the Hydrological Service of Israel. Flow rates in the upper reaches of the river (6000 m upstream) were taken from the Alexander-Elyashiv hydrograph (No. 15120, Hydrological Service of Israel). Sea level and wave height data were taken from the Hadera Meteorarine Monitoring GLOSS station 80 of the Israel Oceanographic and Limnological Research (1-h resolution), 2000 m offshore, ~8 km north of the Alexander River mouth.

Groundwater tidal fluctuations were studied on data subsets with a relatively steady level in order to avoid superimposed signals. A Fourier analysis, carried out on these subsets, produced amplitude and frequency plots. In the plots, the spectrum presented is truncated at 3.5 cpd (cycles per day) and amplified for clarity. The Tsoft package, which is a free software, was used because it enables applying filtering to such Fourier transforms [45].

3. Results

3.1. River Level and Salinity Dynamics

Water level in the Alexander River estuary varied significantly on different time scales, with an overall annual average of 66 cm above sea level (asl) at a distance of 250 m from the sea (Figure 2). During winter, water level showed large fluctuations (hereafter, river events) of up to 110 cm within less than 24 h. Summer fluctuations were smaller (up to 45 cm; Figure 2). In the winter, river events were usually weather-induced, mainly by high sea levels and downriver flood waves. In the summer, the high level was usually built up due to the sandbar at the river mouth, which blocked the base flow to the sea and caused piling up of water behind it. When river level reached sandbar elevation, the sandbar was breached, causing a fast level drop (e.g., Figure 2, 25 May 2013).

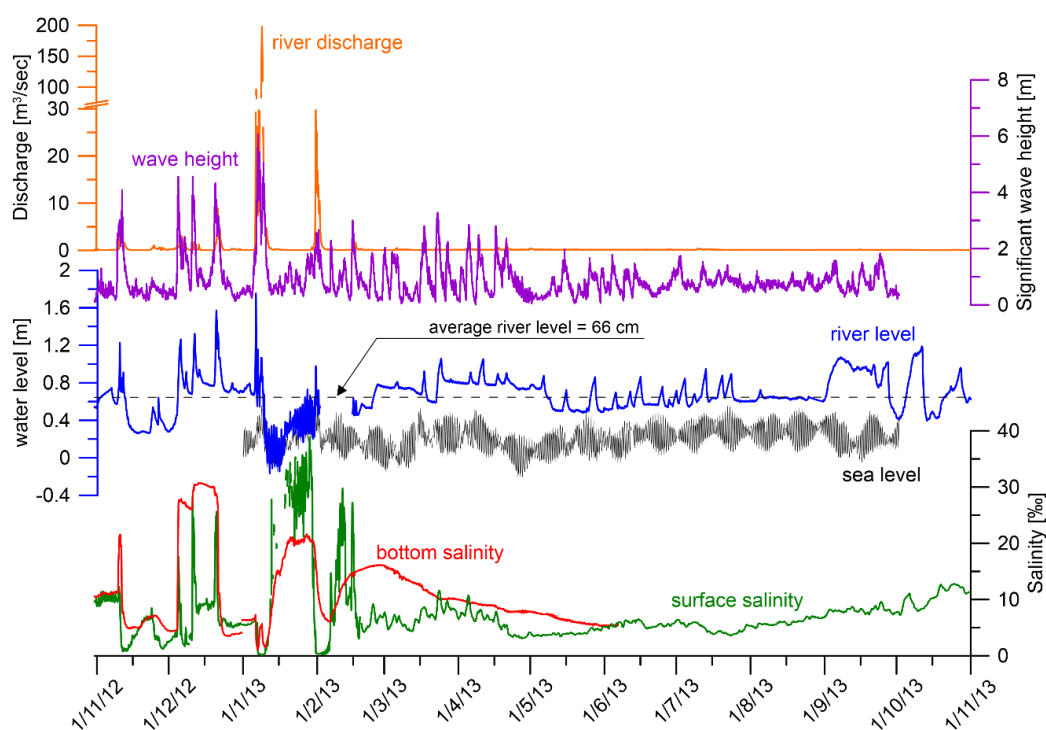


Figure 2. Alexander River discharge, level, and salinity (surface and bottom water, 250 and 500 m, respectively, from the sea). Resolution was at 1 h. Also shown are the sea level from the Hadera Meteorarine Monitoring GLOSS station 80 and the shelf wave height (data from the Israel Oceanography and Limnological Research, IOLR).

River salinity showed large variability (Figure 2). During the winter, the salinity of both surface and deep water varied between 0.1 and 38, where instantaneous salinity changes were associated with river events (Figure 2). While instant increases in salinities are related to high waves ($H_s > 4$ m), decreases in salinity are related to increases in downriver discharge (Figure 2). Between the end of winter (or the last river salinization event) and mid-summer, there was a continuous decrease in deep-water salinity, whereas surface salinity continuously increased.

3.2. Groundwater Dynamics

3.2.1. Groundwater Levels

Groundwater at the Dune site responded coherently to river level fluctuations up to a distance of at least 80 m during both the winter and the summer (Figure 3). Groundwater level changed by up to 70 cm (13–63% of the river level change) in response to winter river events (Figure 4). As a result, hydraulic gradient dipoles changed during these events from toward the river to toward the aquifer (Figure 4b; gradients are hereafter defined as “positive” and “negative”, respectively).

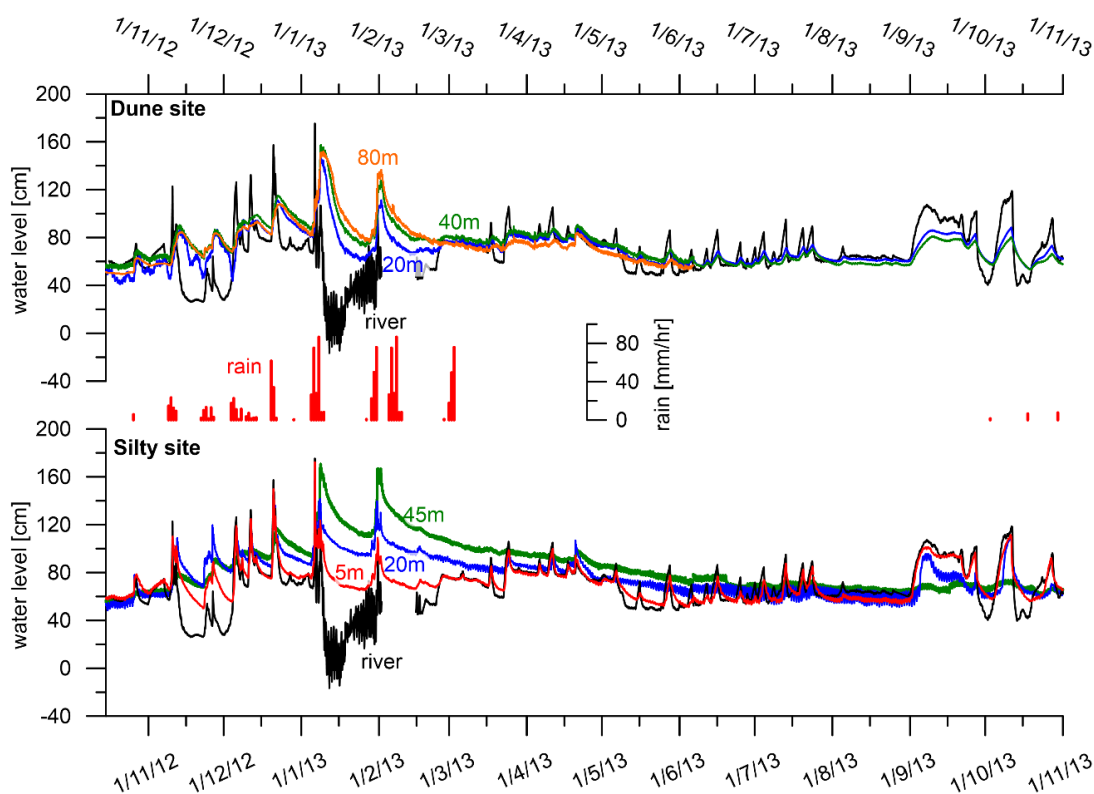


Figure 3. Groundwater levels at the Dune site (top) and at the Silty site (bottom), south and north of the river, respectively, compared with river level. Numbers denote distance in meters from the river. Daily precipitation at 5 km from the sea is also shown (red bars). Short-period zoom-ins are shown in Figure 4.

During winter events, groundwater levels started to rise within a few hours after river level started rising, and their peaks lagged by <24 h at 5 m and by 2–3 days at 20–80 m from the river (Figure 4). Following the peak, levels declined asymptotically and reached base level within 2–3 weeks. Level changes at 20–80 m from the river were almost synchronous, with lags not exceeding several hours (Figure 4b).

During the summer, base groundwater levels were up to 10 cm lower than winter base levels, and gradients varied between slightly positive and zero. During summer river events, groundwater levels

changed by no more than 10 cm, significantly smaller than the corresponding river levels (up to 35 cm), which resulted in short-term (two days) negative gradients (e.g., Figure 5).

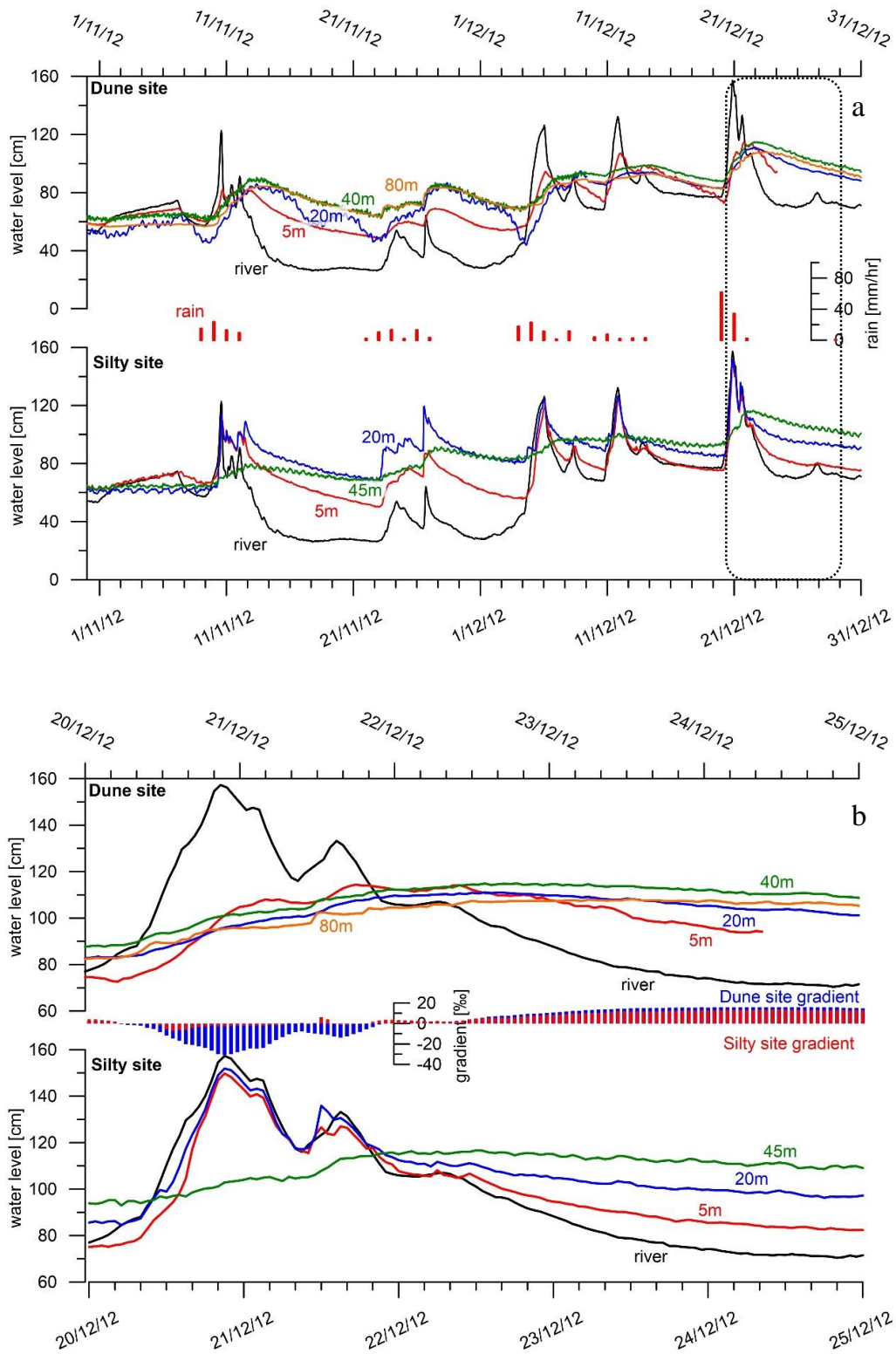


Figure 4. (a) An enlargement of Figure 3 for early winter, 2012. (b) Zoom-in into a single winter river event (late December 2012). Also shown in (b) is the aquifer–river gradient. Numbers denote distance from the river in meters.

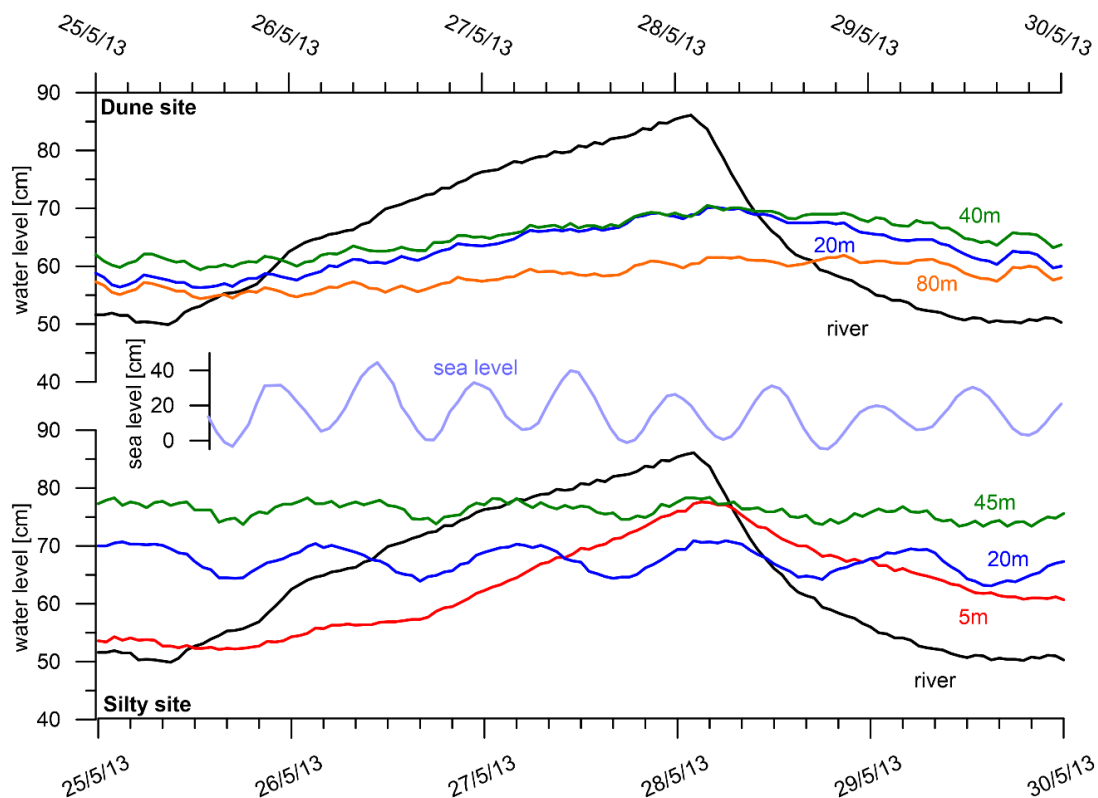


Figure 5. Enlargement of Figure 3 for the response of groundwater to a single summer river event (late May 2013) at sites. Numbers denote distance from the river in meters.

Although less permeable, groundwater at the northern Silty site showed a significant response during winter river events (Figures 3 and 4) both at 5 and 20 m from the river, with fluctuations of up to 100 cm, sometimes similar to those observed in the river (e.g., 5 December 2012 at 5 m from the river, Figure 4a). Moreover, peak levels in the Silty site, both at 5 and 20 m from the river, were recorded almost simultaneously with peak river levels (Figures 3 and 4). On the other hand, summer events seemed to have almost no impact on groundwater level at 20 m, but clearly affected groundwater at 5 m from the river, raising its level by ca. 70% of river level increase (27 and 35 cm, respectively; Figure 5). Decline to base level was asymptotical, but slower than in the Dune site (months; Figure 4). As a result, winter base levels at this site were much higher (up to 30 cm) than in the summer (Figure 3).

Farther away from the river (45 m), where the regional sandy aquifer is exposed, fluctuations were significantly smaller in the winter (Figure 4), with lags usually of 2–3 days, similar to those observed in the sandy Dune site (Figure 4). Summer river events had no impact at this distance.

Diurnal Level Fluctuations

Tidal fluctuations were not observed in river water, except during a short period (~3 weeks) in January 2013, when direct connection was established between the sea and the river for a long enough time (Figure 2). Tidal fluctuations were also hardly observed in groundwater of the Dune site, except for a weak signal of up to 2–3 cm during the summer at 20–80 m from the river (Figure 5). On the other hand, daily cycle fluctuations were clearly observed in the Silty site, mainly during the summer (Figure 5), with amplitudes up to 5 cm in the 20-m borehole. In both sites, fluctuations were hardly observed at 5 m from the river, similar to river water.

3.2.2. Groundwater Salinity

Salinity in the Sandy Dune Site

Salinities of up to 10 were observed in boreholes of the Dune site (Figure 6). While uniform salinity profiles, similar to river surface water (2–8), were typically observed at 5 m from the river, the boreholes at 20–80 m developed a clear fresh–saline water interface (FSI), which slightly deepened between 20 and 40 m from the river (Figure 6). Shallow (<2.5 m depth) groundwater at 20–40 m from the river was mostly fresh (<2), while that of deeper (<3 m asl) groundwater approached ~6–10 (Figure 6). At 80 m from the river, salinities were slightly higher, with shallow and deep water approaching 4 and 10, respectively.

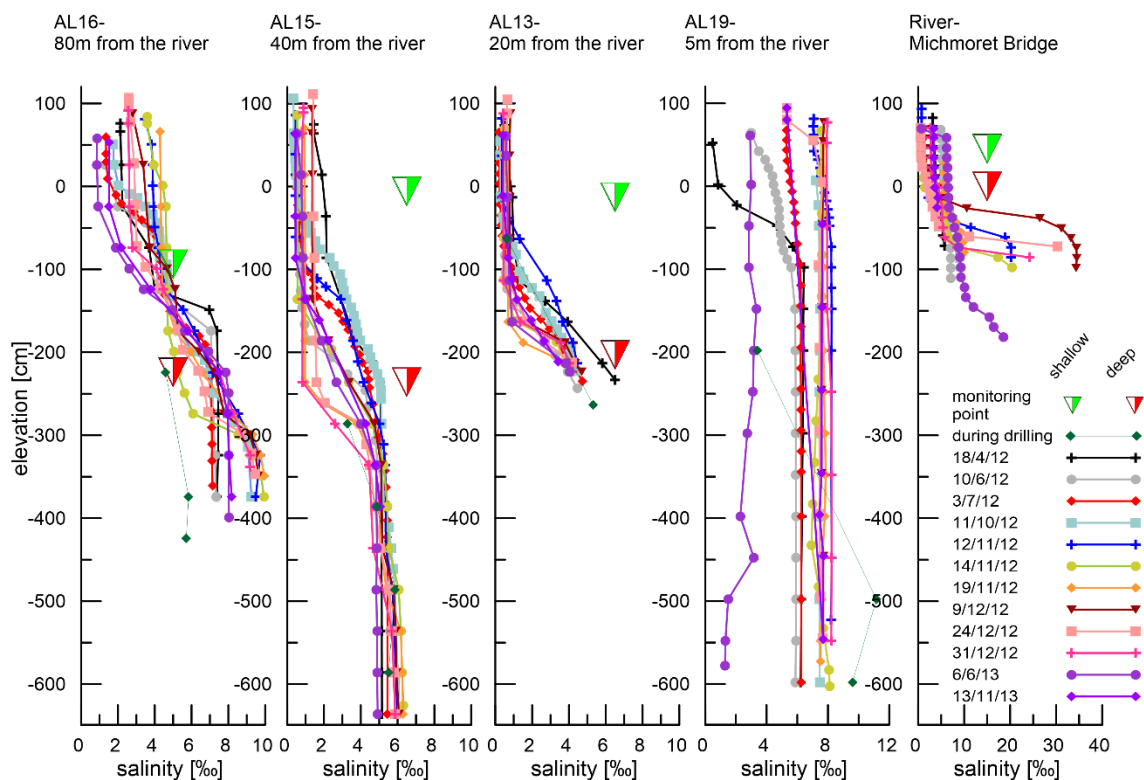


Figure 6. Salinity profiles in the Dune site, compared with river profiles at the Michmoret Bridge, 500 m from the sea. Note the differences in salinity scale. Also shown are the monitoring depths of the monitoring points (data shown in Figure 8).

Fluctuations in FSI depth were observed year-long, although they were larger (up to 2 m) and more frequent during winter events (Figure 7). During winter river events, FSI was usually higher by up to 2 m (reaching 0 m asl, see Figure 8 and monitoring points depth in Figure 6). The FSI rise was almost instantaneous (within 24 h) following river events, with decreasing intensity and increasing time lag with distance from the river (Figure 8). After about two days, the FSI deepened by up to 2 m, at about the same time as groundwater peak level (Figure 8).

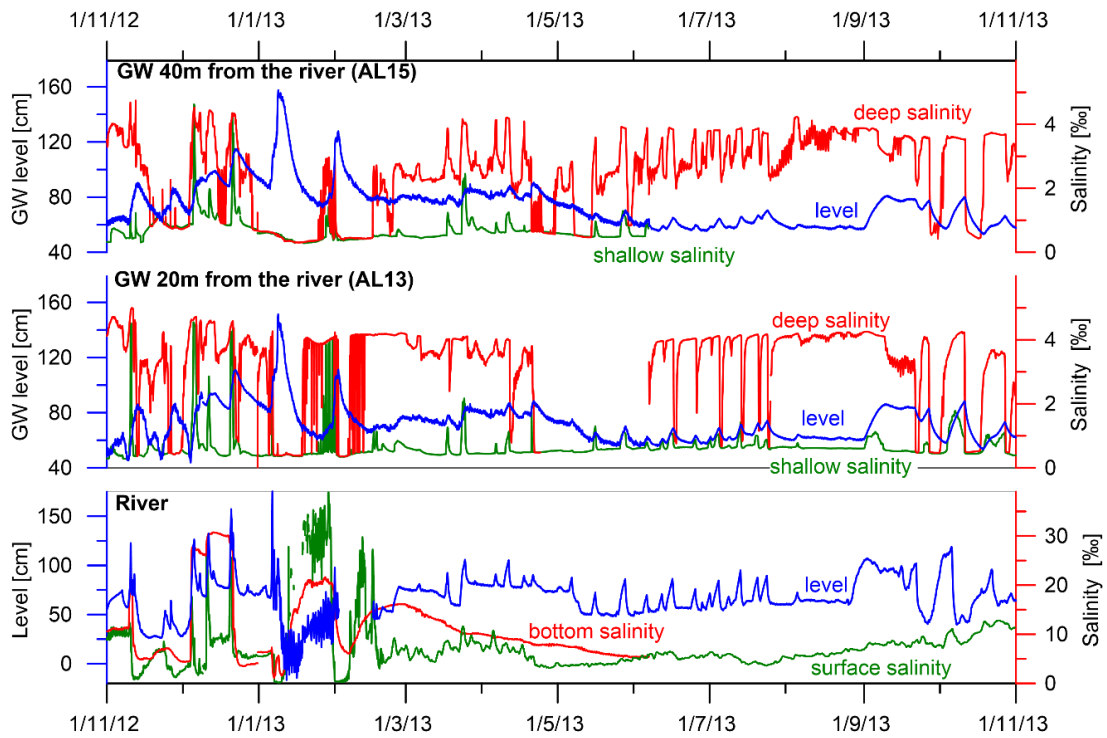


Figure 7. Groundwater level and salinity (1-h resolution) of top and bottom water at the Dune site, 40 m (top) and 20 m (center) from the river, compared with river level and salinity (surface and bottom). Groundwater salinity was measured just above and below the fresh–saline interface (FSI; ~1 m and ~3 m below groundwater level, respectively).

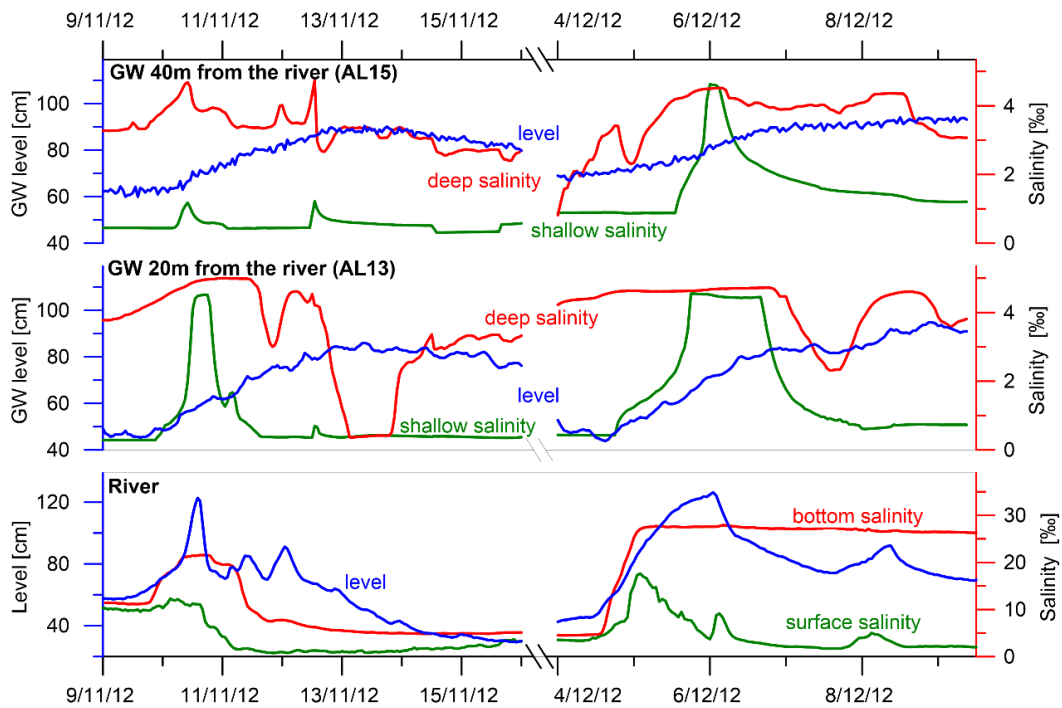


Figure 8. Enlargement of Figure 7, focusing on two river events with different intensities. The first is weaker with a relatively sharp peak and a weak increase in salinity, while the second retains high water level and salinity for several days.

Salinities at the Silty Site

Salinities at the northern, Silty site, up to 20 m from the river, were much higher than in the Dune site (up to 20 and 30 at 20 and 5 m, respectively; Figures 9 and 10). Profiles were quite uniform, with no FSI observed, even during high-salinity events (5 and 20 m from the river, Figure 9). Groundwater salinity was highly variable during early winter, while relatively low during most of the summer (<1 and <6 at 20 and 5 m from the river, respectively, Figure 10). An important observation is that salinity peaks were mainly associated with level peaks in the aquifer and the river (e.g., late October 2012 and September–October 2013, Figure 10), while some major salinity peaks in the river, such as from January to early February 2013, were hardly recorded in groundwater salinity (AL3, 20 m from the river, Figure 10). We also note that the increases in salinity are mostly very sharp (hours to a few days), in particular at the 20 m (AL3) borehole.

In 2012, high salinity (up to 28) was first observed in the Silty site during early October (similarly, in early September 2013) at 5 m from the river (borehole AL6; Figure 10), while, at 20 m, the signal (up to 20) did not appear until late October (borehole AL3; Figure 10). Notably, salinization was hardly observed in the underlying sandy aquifer [16], and at the unit 45 m from the river (up to 1.7; Figure 10).

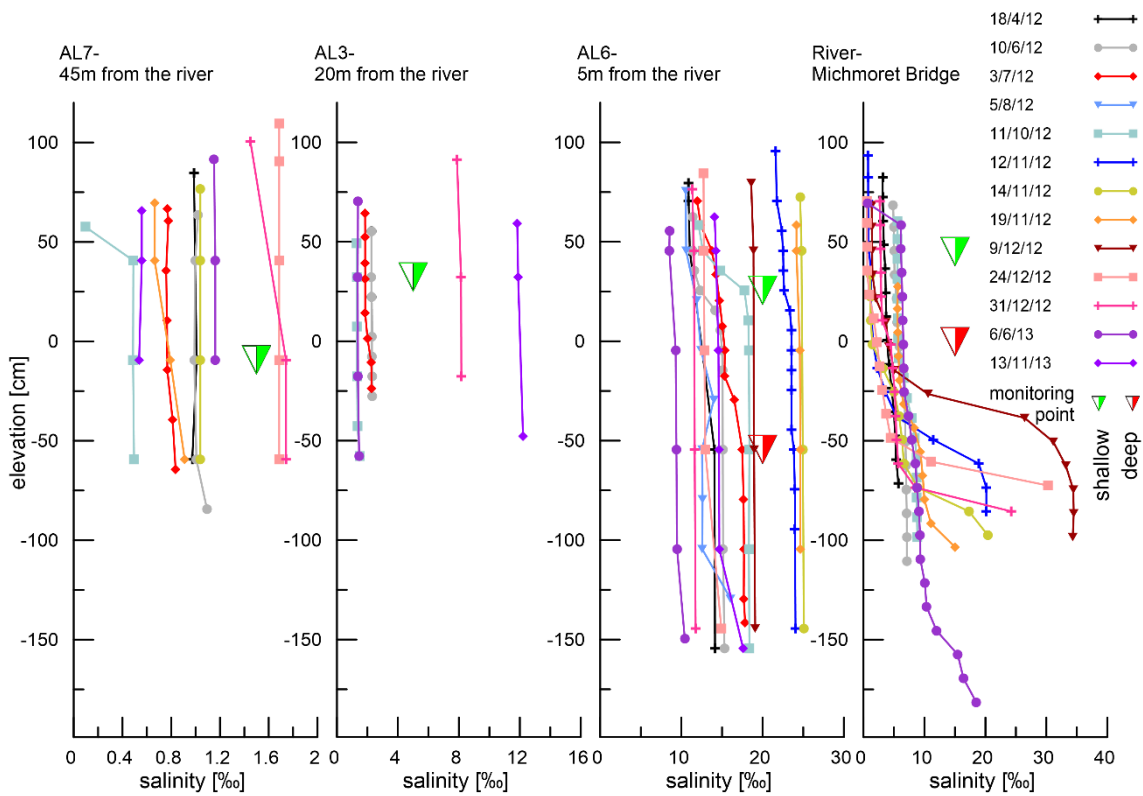


Figure 9. Salinity profiles in boreholes at the Silty site. Note the differences in the salinity scale.

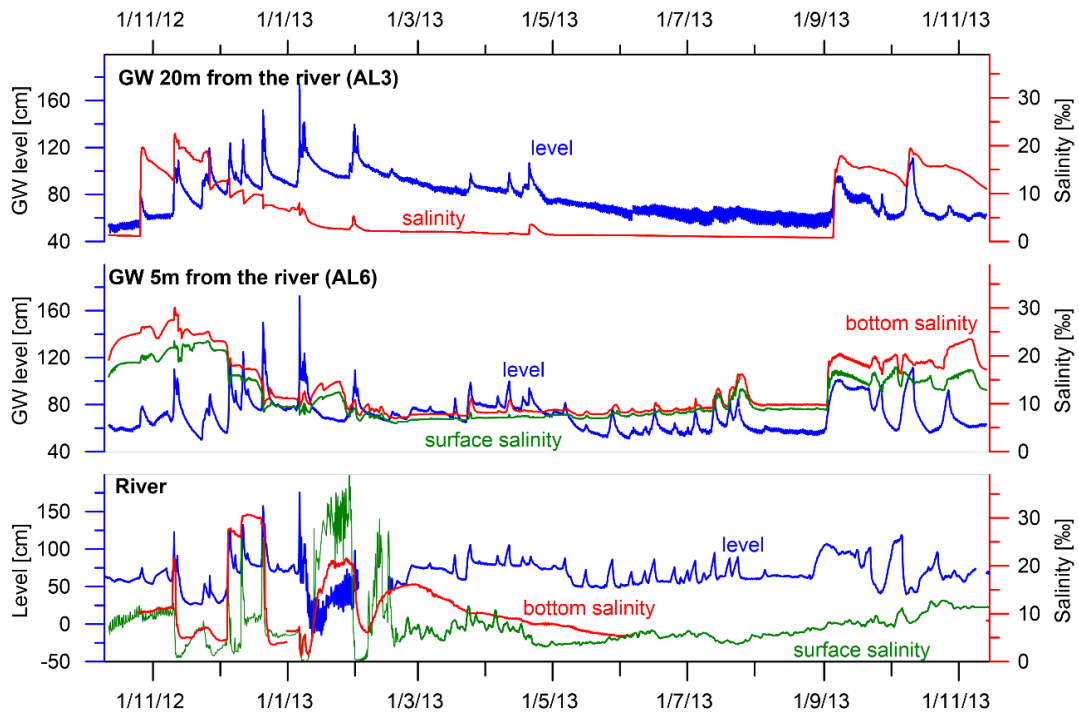


Figure 10. Groundwater level and salinity (1-h resolution) at the Silty site, 20 m (top) and 5 m (center) from the river, compared with river level and salinity.

4. Discussion

Although a small estuarine river, the very frequent changes in levels and salinity in the Alexander River estuary and the different lithologies along its channel allow a detailed investigation of the reaction of an aquifer hydrological system to estuarine dynamics. Whilst both sites along the estuary experience salinization [16], there are large differences in the extent and pattern of salinity between the two sites.

In light of their different lithologies, we suggest below that, while the sandy lithology at the Dune site allows regular circulation of river water in the aquifer, circulation in the clayey silt is much more limited. This allows the accumulation of high-salinity water (Figure 11) in the latter, which is injected into the boreholes through sand lenses that act as conduits during high river stands.

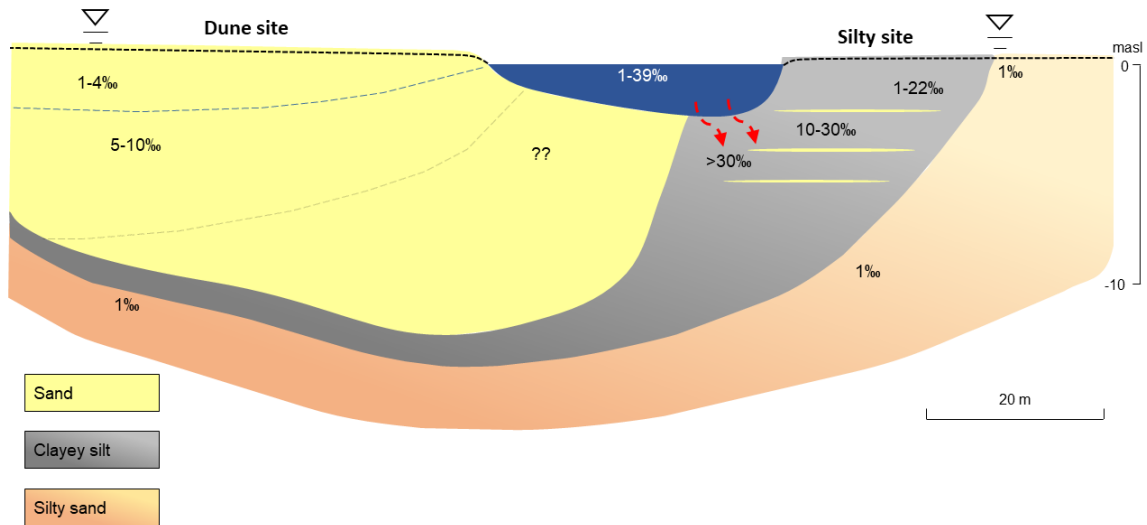


Figure 11. Hydrogeological conceptual model, showing the suggested location of the different water bodies.

4.1. Salinization Patterns in a Sandy Bank

In the sandy Dune site, salinities below the interface were similar to those in the river during non-event periods (4–10, Figures 6 and 7), while higher river salinities (up to >30), documented during seawater encroachment events (days to a few weeks; see Shalem et al. (2014) [16]) were not echoed in higher aquifer salinities. This implies that the time scales involved in the circulation are larger than weeks, which is in agreement with flow rates of a few $\text{m}\cdot\text{yr}^{-1}$, derived for nearby coastal sandy sediments [46,47]. Annual average hydraulic gradients in this site (between the borehole at 40 m from the river and the river itself) were ~ 0.7 toward the river, implying that the river is basically a gaining stream with respect to its sandy banks. Some short-term periods of losing conditions also occur during high-level river events, mainly in the winter (Figure 4b). In borehole AL-19, 5 m from the river, interface was hardly observed (Figure 6), and it should probably be considered as part of the river system.

Typical river events resulted in changes in the depth of the FSI. The immediate reaction to river level rise was a short-term FSI shallowing (see shallow salinity curve in Figure 8). However, this was soon followed by an increase in groundwater level (usually as a response to river level rise), which resulted in a significant deepening of the FSI (Figures 7 and 8; in particular, see the freshening events of January and February 2013), which suggests that the FSI mainly reacted to changes in groundwater head.

4.2. Controls on Salinization in the Silty Bank

Although salinity at the Silty site may decrease to almost fresh water at 20 m from the river, (Figure 10; see also Shalem et al. 2014 [16]), high salinity (up to 36 at 5 m and 22 at 20 m) was very often observed in this site, including both long periods (end of summer to beginning of winter, mainly at 5 m from the river) and salinization “events”, which were more common during the winter (Figure 10).

The most striking observation is that groundwater of this site often reached salinities significantly higher than in the river. This is true most of the time for 5 m from the river, while common during winter also at 20 m from the river (Figure 10). This suggests that saline groundwater in this site does not represent current river water circulation in the aquifer but, rather, it possibly represents larger, probably longer, past seawater encroachment in the river channel. Nevertheless, the salinity pattern in this unit is clearly a reflection on changes in current river water level, reacting to both short-term and long-term changes in the hydraulic gradient between the river and the silty aquifer (Figure 12). This can be identified, for example, in the large increase in salinity in October 2012 and in the abrupt increase in salinity at both boreholes in September 2013 (Figure 12), which followed a relatively fast river level rise and a change to a negative gradient, while river water salinity was relatively low and showed no salinization event (Figure 10). There are also numerous salinity peaks, which respond almost instantaneously (commonly <1 h) to high-level river events, which usually create short-term changes to negative gradients (Figure 12). These peaks/events are very common during the rainy season (winter), but summer events are also common, mostly limited to the 5-m borehole. Noteworthy, changes in groundwater salinity, associated with river events, include both rises and drops in groundwater salinity (Figure 12; e.g., 27 November and 20 December 2012), depending on the aquifer-river gradient direction at the time of the event.

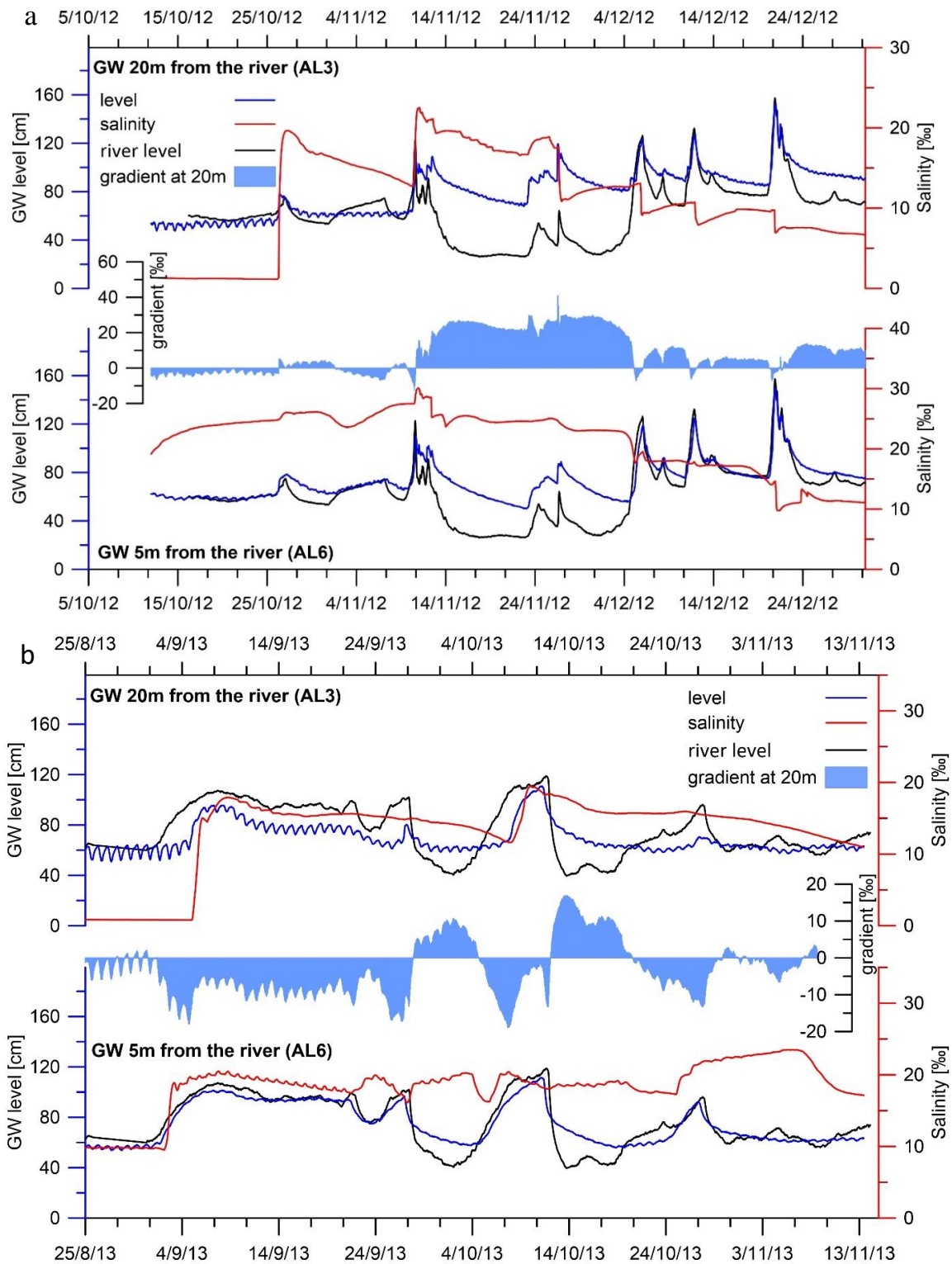


Figure 12. Groundwater level and salinity, and aquifer–river gradient during (a) fall 2012 and (b) fall 2013.

The above observations are best explained by the long-term presence of saline water body or bodies in the clayey silt (Figure 11), probably remnants of past long-term seawater encroachment in the river channel, and by the frequent migration of this water within the aquifer due to head changes. We suggest that it is the sand lenses within the clayey silt (Figure 11) that allow this migration, i.e., the

lenses function as conduits, while the silt behaves as a confining layer. The high hydraulic diffusivity (low storativity) of these confined lenses allow the efficient propagation of the pressure signal and the almost instantaneous “injection” of saline water into the boreholes (Figures 10 and 12). It seems that, while following relatively high river stands (close to zero or negative gradients), changes in level result in the injection of saline water through the lenses and increase in borehole salinity, whereby changes that follow positive gradients (higher levels in the aquifer) tend to result in a salinity decline due to level increase (Figure 12). This reflects on the local nature of the high-salinity water pockets, and probably also on the small size of the sandy lens conduits.

Similar fast propagation of the pressure signal, with little attenuation, was described in non-uniform aquifer units from the Sandy Creek estuary, Australia [48]. These results are also consistent with other studies that showed that, in lower-storativity aquifer units, the groundwater reaction to a flood wave is more intense [49,50]. We note that degradation of plant roots, which are common in this site, could create macro-pores, which could also aid in the migration of the saline water [51].

The mostly uniform profiles (i.e., no interface) observed at 5 and 20 m from the river are more difficult to explain. We suggest that this is a borehole artefact, induced by a vertical flow in the long perforated borehole, which could enhance EC fluctuations by orders of magnitude, as shown by Levanon et al. (2013) [52] for tidal fluctuations in a coastal aquifer. Boreholes may act as a short circuit along a vertical gradient, connecting between the higher and lower hydraulic head zones. As a result, flow in the well is often large enough to compromise the integrity of water samples [53].

Shalem et al. (2014) [16] showed by resistivity measurements that there is saline water in the sediments beneath the river (down to ca. 10 m depth; Figure 11). This saline water could be constrained at the sub-river or extend to some distance off-river in the clayey silt, where it could mix with some lower-salinity water (Figure 11). Whatever its exact location is, we suggest that, during high river stand, the saline water is being pushed through the sand lenses off-river and up into the boreholes, aided by the borehole flow effect.

On the other hand, both our observations and ERT (Electrical Resistance Tomography) resistivity transect, presented by Shalem et al. (2014) [16], show no indication for saline water in the sand aquifer at 45 m and beneath the silt unit. This is the result of both the hydraulic disconnectivity with the river (applied by the silt), as well as the lack of confinement, which suppresses the pressure signal and, therefore, does not favor migration of saline water farther off-river.

Tidal Signals in Groundwater

Tidal fluctuations were hardly observed in the Alexander River estuary (Figures 2 and 13), probably due to its typical condition of disconnection from the sea by the sandbar. On the other hand, tidal fluctuations were clearly observed in the clayey silt unit (up to 13 cm, Figures 13 and 14), in particular during the summer (Figures 5 and 14), suggesting the existence of a tidal forcing, which is not through the adjacent river. The Silty site is located 300 m from the sea and is a local unit, not connected to the sea. Therefore, there is no reason to assume that the tidal forcing here is induced by the sea. This is also supported by the very weak diurnal tidal signal in this site (Figure 13).

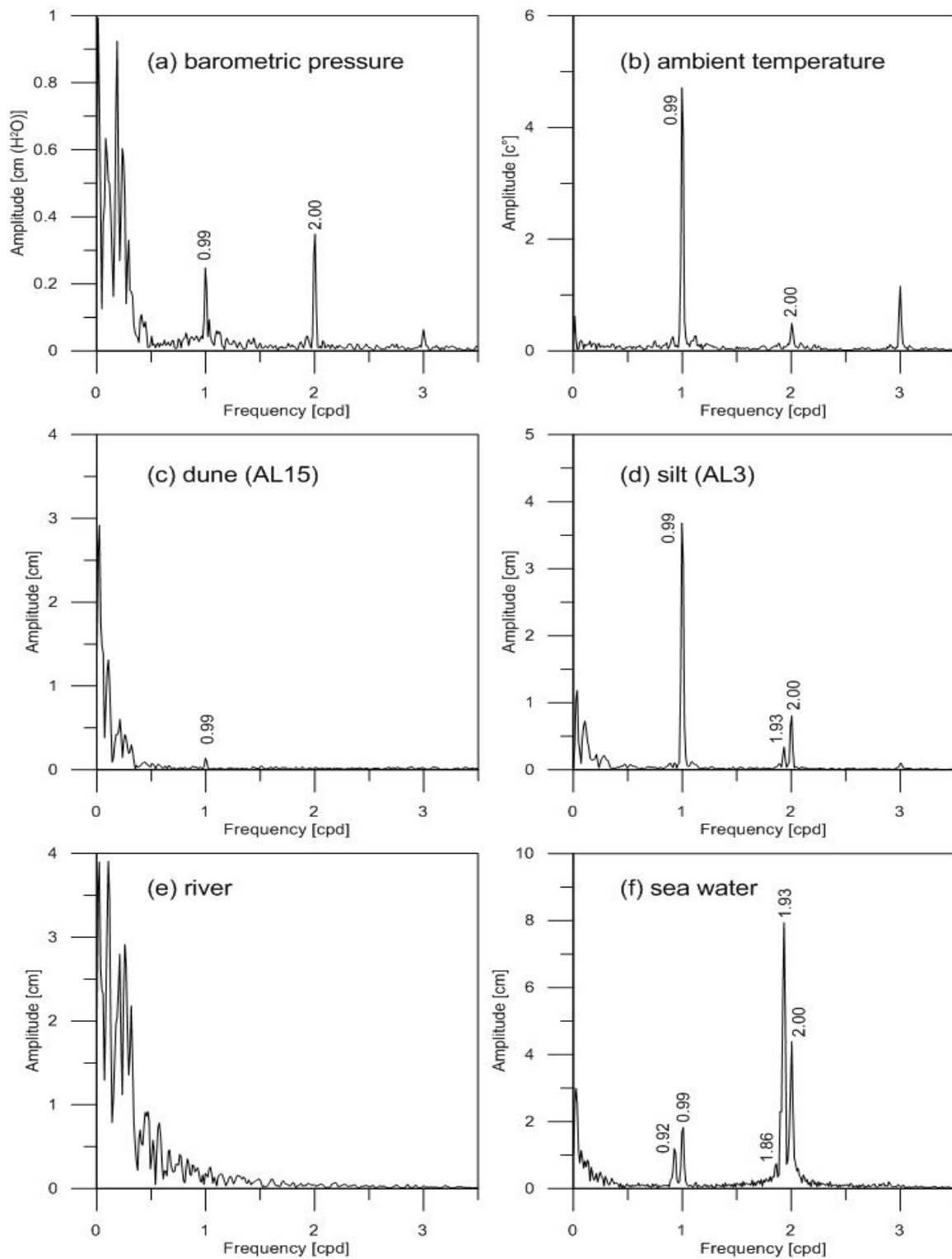


Figure 13. Fourier analysis of the May–August 2013 datasets of (a) barometric pressure, (b) relative ambient temperature, (c) groundwater level in the dune unit (40 m from the river), (d) groundwater level in the clayey silt unit (20 m from the river), (e) river water level, and (f) seawater from the Hadera Meteorological Monitoring GLOSS station 80.

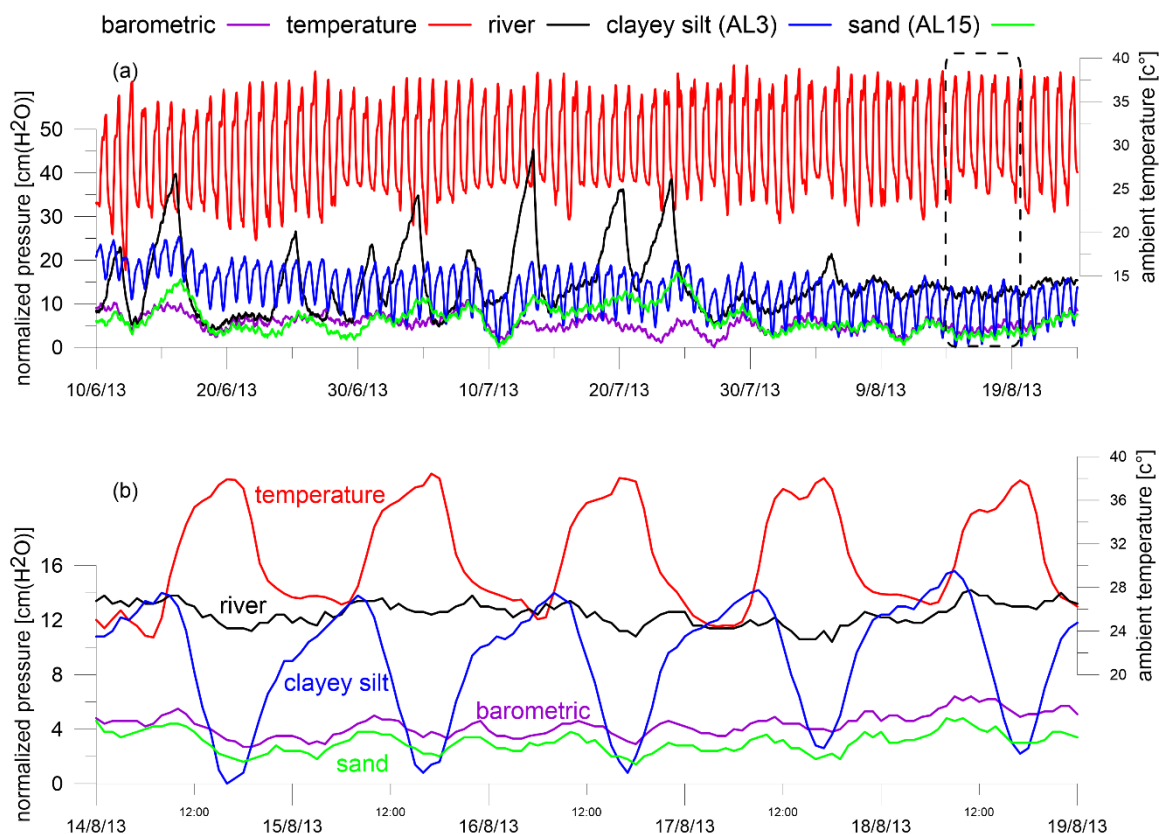


Figure 14. Groundwater level tidal fluctuations at the silty site, compared with groundwater level at the sandy site, and river, as well barometric pressure and temperature. Barometric pressure is normalized to 0 cm (above mesa level). (b) Enlargement of the dashed rectangle in the top panel (a).

A Fourier analysis was carried out on a subset of data between May and August 2013 (Figure 13). Amplitudes in the clayey silt groundwater were very prominent, while hardly identified in the dune groundwater (Figure 13). The most dominant frequency was 1 cpd (day^{-1}), with an amplitude of 3.8 cm (Figure 13). The other two frequencies were 1.93 and 2 cpd, with much smaller amplitudes of 0.3 and 0.8 cm, respectively (Figure 13). The 1-cpd frequency pattern shows a negative correlation with that of the ambient temperature frequency (Figures 13 and 14). This suggests that water pressure falls as soon as the ambient temperature begins to rise in the morning and recovers after sunset (Figure 14b). This complies with other observations from the literature [6,54,55] and can be explained by the photosynthetic demand of water by plants during the daytime, which acts like a cyclic pump [6,54,55]. Moreover, the 1-cpd amplitude increases with the seasonal increase in average daily temperature, from <3 cm during winter up to 13 cm in summer (Figure 10), which is in accordance with the increase in photosynthetic demand [54]. The tidal amplitude observed in our study is larger than in other studies (13 cm compared with 9 and 4 cm, respectively, in Acworth et al. (2014) and Butler et al. (2007) [6,54]), which could be related to different vegetation types [56]. The boreholes in the Silty unit are located next to thick vegetation, and roots were found at depth during drilling, while there is hardly any vegetation in the Dune site. Accordingly, daily tidal fluctuations were hardly observed in the latter even during the summer (Figure 14). Other processes suggested in the literature for similar cases of diurnal cycles are losing streams [57], daily precipitation in a tropical area [58], and freezing–thawing processes [55]. However, none of these processes fit the Alexander River environment.

The decrease in tidal amplitude toward the river channel (smaller at 5 than at 20 m; Figure 5) may be attributed to the better connection with the river, which could mask the signal [54,59]. This could also be due to the lower extent of vegetation adjacent to the river in this area.

4.3. Conclusions

Seawater intrusion via estuarine rivers is site-dependent and highly dependent on subsurface heterogeneity and hydraulic gradient. While, in other locations with different hydrogeology settings, aquifer salinization pattern may act different, for a similar setting as the Alexander Estuary, we draw the following conclusions:

1. The interaction of an estuarine river with a high-permeability aquifer, such as at the Dune site, is similar to common coastal settings, including the formation of a quasi-steady-state FSI.
2. Low-permeability aquifer units may store high-salinity water, remnants of past seawater encroachment in the river channel.
3. The sharp fluctuations in salinity, observed in the Alexander River Silty site in relation to river events are due to (1) the occurrence of saline water bodies in this unit, (2) changes in river water levels, and (3) the existence of high-permeability lenses with low storativity within the silt.
4. The low-permeability unit is efficiently blocking the saline water from reaching the regional sandy aquifer, even at a short distance from the river.
5. Daily fluctuations in the Silty unit, which negatively correlate with solar radiation, are probably due to a photosynthetic pump.

Author Contributions: Conceptualization, Y.S., Y.Y., B.H. and Y.W.; methodology, Y.S., Y.Y., B.H. and Y.W. and Y.Y.; validation, Y.Y., B.H. and Y.W.; investigation, Y.S., Y.Y., B.H. and Y.W.; resources, Y.Y., B.H. and Y.W.; writing—original draft preparation, Y.S., Y.Y. and Y.W.; writing—review and editing, Y.S., Y.Y., B.H. and Y.W.; visualization, Y.S.; supervision, Y.Y., B.H. and Y.W.; project administration, Y.Y., B.H. and Y.W.; funding acquisition, Y.Y., B.H. and Y.W.

Funding: This research was funded by the Israel Science Foundation grant No. 1527/2008. The first author is also grateful to the Israel Ministry of Science for granting him the Eshkol scholarship.

Acknowledgments: The authors wish to thank Hallel Lotzky, Iyad Swaed, Yoav Boaz, Alon Moshe, Yael Neumeier, Yona Geler, Avishai Abbo, Elisheva Refaeli, Yakov Mizrachi, Chaim Hemo, and Shlomo Askenazi from the Geological Survey of Israel and the Hebrew University for their help in the field and lab work. We owe gratitude to Dov S. Rosen and Lazar Raskin from the Israel Oceanography and Limnological Research (IOLR) Institute for providing data on sea level and wave height, and to Yaron Gertner (IOLR) for his assistance in the field. We also wish to thank Yariv Malichi, David Keren, and Eran Starous from the Israel Nature and Parks Authority for issuing the work permits for the Alexander River. This work was supported by the Israel Science Foundation grant No. 1527/2008. The first author is also grateful to the Israel Ministry of Science for granting him the Eshkol scholarship.

Conflicts of Interest: The authors declare no conflict of interest.

References

1. Conrads, P.; Roehl, E.; Daamen, R.; Cook, J.; Sexton, C.T.; Water, B.J.; Authority, S.; Tufford, D.L.; Carbone, G.J.; Dow, K. Estimating salinity intrusion effects due to climate change on the lower savannah river estuary. In Proceedings of the South Carolina Environmental Conference, Myrtle Beach, SC, USA, 10–13 March 2019; p. 8.
2. Demirel, Z. The history and evaluation of saltwater intrusion into a coastal aquifer in Mersin, Turkey. *J. Environ. Manag.* **2004**, *70*, 275–282. [[CrossRef](#)] [[PubMed](#)]
3. Green, T.R.; Taniguchi, M.; Kooi, H.; Gurdak, J.J.; Allen, D.M.; Hiscock, K.M.; Treidel, H.; Aureli, A. Beneath the surface of global change: Impacts of climate change on groundwater. *J. Hydrol.* **2011**, *405*, 532–560. [[CrossRef](#)]
4. Kåss, A.; Gavrieli, I.; Yechieli, Y.; Vengosh, A.; Starinsky, A. The impact of freshwater and wastewater irrigation on the chemistry of shallow groundwater: A case study from the Israeli Coastal Aquifer. *J. Hydrol.* **2005**, *300*, 314–331. [[CrossRef](#)]
5. Sherif, M.M.; Singh, V.P. Effect of climate change on sea water intrusion in coastal aquifers. *Hydrol. Process.* **1999**, *13*, 1277–1287. [[CrossRef](#)]
6. Acworth, R.I.; Rau, G.C.; McCallum, A.M.; Andersen, M.S.; Cuthbert, M.O. Understanding connected surface-water/groundwater systems using Fourier analysis of daily and sub-daily head fluctuations. *Hydrogeol. J.* **2014**, *23*, 143–159. [[CrossRef](#)]
7. Cooper, H.H. A hypothesis concerning the dynamic balance of fresh water and salt water in a coastal aquifer. *J. Geophys. Res. Space Phys.* **1959**, *64*, 461–467. [[CrossRef](#)]

8. Moore, W.S. Large groundwater inputs to coastal waters revealed by ^{226}Ra enrichments. *Nature* **1996**, *380*, 612–614. [[CrossRef](#)]
9. Weinstein, Y.; Burnett, W.C.; Swarzenski, P.W.; Shalem, Y.; Yechieli, Y.; Herut, B. Role of aquifer heterogeneity in fresh groundwater discharge and seawater recycling: An example from the Carmel coast, Israel. *J. Geophys. Res. Space Phys.* **2007**, *112*, C12016. [[CrossRef](#)]
10. Bear, J.; Cheng, A.H.D.; Sorek, S.; Ouazar, D.; Herrera, I. *Seawater Intrusion in Coastal Aquifers: Concepts, Methods, and Practices*; Kluwer Academic Publishers: London, UK, 1999; p. 627.
11. Oz, I.; Shalev, E.; Gvirtzman, H.; Yechieli, Y.; Gavrieli, I. Groundwater flow patterns adjacent to a long-term stratified (meromictic) lake. *Water Resour. Res.* **2011**, *47*, 47. [[CrossRef](#)]
12. Post, V.E.A. Fresh and saline groundwater interaction in coastal aquifers: Is our technology ready for the problems ahead? *Hydrogeol. J.* **2005**, *13*, 120–123. [[CrossRef](#)]
13. Van Dam, J.C. Exploitation, Restoration and Management. In *Seawater Intrusion in Coastal Aquifers—Concepts, Methods and Practices*; Bear, J., Ed.; Kluwer Academic Publishers: London, UK, 1999; pp. 73–125.
14. Acworth, R.I.; Dasey, G.R. Mapping of the hyporheic zone around a tidal creek using a combination of borehole logging, borehole electrical tomography and cross-creek electrical imaging, New South Wales, Australia. *Hydrogeol. J.* **2003**, *11*, 368–377. [[CrossRef](#)]
15. Linderfelt, W.R.; Turner, J.V. Interaction between shallow groundwater, saline surface water and nutrient discharge in a seasonal estuary: The Swan-Canning system. *Hydrol. Process.* **2001**, *15*, 2631–2653. [[CrossRef](#)]
16. Shalem, Y.; Weinstein, Y.; Levi, E.; Herut, B.; Goldman, M.; Yechieli, Y. The extent of aquifer salinization next to an estuarine river: An example from the eastern Mediterranean. *Hydrogeol. J.* **2014**, *23*, 69–79. [[CrossRef](#)]
17. Sivan, O.; Yechieli, Y.; Herut, B.; Lazar, B. Geochemical evolution and timescale of seawater intrusion into the coastal aquifer of Israel. *Geochim. Cosmochim. Acta* **2005**, *69*, 579–592. [[CrossRef](#)]
18. Vengosh, A.; Rosenthal, E. Saline groundwater in Israel: Its bearing on the water crisis in the country. *J. Hydrol.* **1994**, *156*, 389–430. [[CrossRef](#)]
19. Ataie-Ashtiani, B.; Volker, R.; Lockington, D. Tidal effects on sea water intrusion in unconfined aquifers. *J. Hydrol.* **1999**, *216*, 17–31. [[CrossRef](#)]
20. Melloul, A.J.; Zeitoun, D.G. A Semi-Empirical Approach to Intrusion Monitoring in Israeli Coastal Aquifer. In *Seawater Intrusion in Coastal Aquifers: Concepts, Methods and Practices*; Bear, J., Ed.; Kluwer Academic Publishers: London, UK, 1999; pp. 543–558.
21. Robinson, C.; Gibbes, B.; Carey, H.; Li, L. Salt-freshwater dynamics in a subtterranean estuary over a spring-neap tidal cycle. *J. Geophys. Res. Space Phys.* **2007**, *112*, 1–15. [[CrossRef](#)]
22. Zhang, Y.; Li, L.; Erler, D.V.; Santos, I.; Lockington, D. Effects of beach slope breaks on nearshore groundwater dynamics. *Hydrol. Process.* **2017**, *31*, 2530–2540. [[CrossRef](#)]
23. Goldman, M.; Gilad, D.; Ronen, A.; Melloul, A. Mapping of seawater intrusion into the coastal aquifer of Israel by the time domain electromagnetic method. *GeosExploration* **1991**, *28*, 153–174. [[CrossRef](#)]
24. Swarzenski, P.W.; Burnett, W.C.; Greenwood, W.J.; Herut, B.; Peterson, R.; Dimova, N.; Shalem, Y.; Yechieli, Y.; Weinstein, Y. Combined time-series resistivity and geochemical tracer techniques to examine submarine groundwater discharge at Dor Beach, Israel. *Geophys. Res. Lett.* **2006**, *33*, L24405. [[CrossRef](#)]
25. Freeze, R.A.; Cherry, J.A. *Groundwater*; Prentice-Hall: Englewood Cliffs, NJ, USA, 1979; p. 604.
26. Michael, H.A.; Mulligan, A.E.; Harvey, C.F. Seasonal oscillations in water exchange between aquifers and the coastal ocean. *Nature* **2005**, *436*, 1145–1148. [[CrossRef](#)] [[PubMed](#)]
27. Faye, S.; Maloszewski, P.; Stichler, W.; Trimborn, P.; Cissé Faye, S.; Bécaye Gaye, C. Groundwater salinization in the Saloum (Senegal) delta aquifer: Minor elements and isotopic indicators. *Sci. Total Environ.* **2005**, *343*, 243–259. [[CrossRef](#)] [[PubMed](#)]
28. Murgulet, D.; Tick, G. The extent of saltwater intrusion in Southern Baldwin County, Alabama. *Environ. Geol.* **2008**, *55*, 1235–1245. [[CrossRef](#)]
29. Ngom, F.; Tweed, S.; Bader, J.-C.; Saos, J.-L.; Malou, R.; LeDuc, C.; Leblanc, M. Rapid evolution of water resources in the Senegal delta. *Glob. Planet. Chang.* **2016**, *144*, 34–47. [[CrossRef](#)]
30. Navoy, A.S.; Voronin, L.M.; Modica, E. *Vulnerability of Production Wells in the Potomac-Raritan-Magothy Aquifer System to Saltwater Intrusion from the Delaware River in Camden, Gloucester, and Salem Counties, New Jersey*; US Department of the Interior, US Geological Survey: Leston, VA, USA, 2005.
31. Smith, A.J.; Turner, J.V. Density-dependent surface water-groundwater interaction and nutrient discharge in the Swan-Canning Estuary. *Hydrol. Process.* **2001**, *15*, 2595–2616. [[CrossRef](#)]

32. Findlay, S. Importance of surface-subsurface exchange in stream ecosystems: The hyporheic zone. *Limnol. Oceanogr.* **1995**, *40*, 159–164. [[CrossRef](#)]
33. Hayashi, M.; Rosenberry, D.O. Effects of Ground Water Exchange on the Hydrology and Ecology of Surface Water. *Ground Water* **2002**, *40*, 309–316. [[CrossRef](#)] [[PubMed](#)]
34. Williams, D.D. Nutrient and flow vector dynamics at the hyporheic/groundwater interface and their effects on the interstitial fauna. *Hydrobiologia* **1993**, *251*, 185–198. [[CrossRef](#)]
35. Glover, R.E. The pattern of fresh-water flow in a coastal aquifer. *J. Geophys. Res. Space Phys.* **1959**, *64*, 457–459. [[CrossRef](#)]
36. Lenkopane, M.; Werner, A.D.; Lockington, D.A.; Li, L. Influence of variable salinity conditions in a tidal creek on riparian groundwater flow and salinity dynamics. *J. Hydrol.* **2009**, *375*, 536–545. [[CrossRef](#)]
37. Reilly, T.E.; Goodman, A.S. Quantitative analysis of saltwater-freshwater relationships in groundwater systems—A historical perspective. *J. Hydrol.* **1985**, *80*, 125–160. [[CrossRef](#)]
38. Werner, A.D.; Lockington, D.A. Tidal impacts on riparian salinities near estuaries. *J. Hydrol.* **2006**, *328*, 511–522. [[CrossRef](#)]
39. Trefry, M.; Svensson, T.; Davis, G. Hypo- and hyper-saline influences on groundwater flux to a seasonally saline river. *J. Hydrol.* **2007**, *335*, 330–353. [[CrossRef](#)]
40. Sarig, G. *The Suspected Influence of Seawater Drainage from Sea Turtle Rescue Center on the Ecological System of the Alexander Estuary*; Rupin Academic Center: Michmoret, Israel, 2008; p. 32.
41. Gvirtzman, G.; Wieder, M. Climate of the last 53,000 Years in the eastern Mediterranean, based on soil-sequence Stratigraphy in the coastal plain of Israel. *Quat. Sci. Rev.* **2001**, *20*, 1827–1849. [[CrossRef](#)]
42. Lichter, M. *The Dynamic Morphology of River Mouths along the Mediterranean Coast of Israel*; Haifa University: Haifa, Israel, 2009.
43. Lichter, M.; Klein, M.; Zviely, D. Dynamic morphology of small south-eastern Mediterranean river mouths: A conceptual model. *Earth Surf. Process. Landf.* **2011**, *36*, 547–562. [[CrossRef](#)]
44. Lewis, E.L. The practical salinity scale of 1978 and its antecedents. *Mar. Geodesy* **1982**, *5*, 350–357. [[CrossRef](#)]
45. Van Camp, M.; Vauterin, P. Tsoft: Graphical and interactive software for the analysis of time series and Earth tides. *Comput. Geosci.* **2005**, *31*, 631–640. [[CrossRef](#)]
46. Gvirtzman, H.; Magaritz, M. Investigation of Water Movement in the Unsaturated Zone Under an Irrigated Area Using Environmental Tritium. *Water Resour. Res.* **1986**, *22*, 635–642. [[CrossRef](#)]
47. Ronen, D.; Magaritz, M.; Paldor, N.; Bachmat, Y. The Behavior of Groundwater in the Vicinity of the Water Table Evidenced by Specific Discharge Profiles. *Water Resour. Res.* **1986**, *22*, 1217–1224. [[CrossRef](#)]
48. Carey, H.; Lenkopane, M.K.; Werner, A.D.; Li, L.; Lockington, D.A.; Werner, A. Tidal controls on coastal groundwater conditions: Field investigation of a macrotidal system. *Aust. J. Earth Sci.* **2009**, *56*, 1165–1179. [[CrossRef](#)]
49. Barlow, P.; DeSimone, L.; Moench, A. Aquifer response to stream-stage and recharge variations. II. Convolution method and applications. *J. Hydrol.* **2000**, *230*, 211–229. [[CrossRef](#)]
50. Moench, A.F.; Barlow, P.M. Aquifer response to stream-stage and recharge variations. I. Analytical step-response functions. *J. Hydrol.* **2000**, *230*, 192–210. [[CrossRef](#)]
51. Xin, P.; Kong, J.; Li, L.; Barry, D.; Barry, D. Effects of soil stratigraphy on pore-water flow in a creek-marsh system. *J. Hydrol.* **2012**, *475*, 175–187. [[CrossRef](#)]
52. Levanon, E.; Yechieli, Y.; Shalev, E.; Friedman, V.; Gvirtzman, H. Reliable Monitoring of the Transition Zone Between Fresh and Saline Waters in Coastal Aquifers. *Ground Water Monit. Remediat.* **2013**, *33*, 101–110. [[CrossRef](#)]
53. Shalev, E.; Lazar, A.; Wollman, S.; Kington, S.; Yechieli, Y.; Gvirtzman, H. Biased Monitoring of Fresh Water-Salt Water Mixing Zone in Coastal Aquifers. *Ground Water* **2009**, *47*, 49–56. [[CrossRef](#)]
54. Butler, J.J.; Kluitenberg, G.J.; Whittlemore, D.O.; Loheide, S.P.; Jin, W.; Billinger, M.A.; Zhan, X. A field investigation of phreatophyte-induced fluctuations in the water table. *Water Resour. Res.* **2007**, *43*, W02404. [[CrossRef](#)]
55. Gribovszki, Z.; Szilágyi, J.; Kalicz, P. Diurnal fluctuations in shallow groundwater levels and streamflow rates and their interpretation—A review. *J. Hydrol.* **2010**, *385*, 371–383. [[CrossRef](#)]
56. Thal-Larsen, J.H. Fluctuations in the level of the phreatic surface with an atmospheric deposit in the form of dew. *Bodenkd. Forsch.* **1935**, *4*, 223–233.

57. Cayan, D.R.; Lundquist, J.D. Seasonal and Spatial Patterns in Diurnal Cycles in Streamflow in the Western United States. *J. Hydrometeorol.* **2002**, *3*, 591–603.
58. Wain, A. Diurnal River Flow Variations and Development Planning in the Tropics. *Geogr. J.* **1994**, *160*, 295–306. [[CrossRef](#)]
59. Johnson, B.; Malama, B.; Barrash, W.; Flores, A.N. Recognizing and modeling variable drawdown due to evapotranspiration in a semiarid riparian zone considering local differences in vegetation and distance from a river source. *Water Resour. Res.* **2013**, *49*, 1030–1039. [[CrossRef](#)]



© 2019 by the authors. Licensee MDPI, Basel, Switzerland. This article is an open access article distributed under the terms and conditions of the Creative Commons Attribution (CC BY) license (<http://creativecommons.org/licenses/by/4.0/>).